ACS OMEGA

http://pubs.acs.org/journal/acsodf

Article

Performance Evaluation of an Octadecyltrimethyl Ammonium Chloride−Dimethyl Silicone Oil as a Waterproof Locking Agent in Low-Permeability Reservoirs

Xiaolong Zhao,* Miao Liu, Cheng Ma,* Chen Wang, Jiang Yang, Chao Yang, and Zhongwei Sun

Cite This: *ACS Omega* 2022, 7, 31954−31960

Read Online

ACCESS | Metrics & More | Article Recommendations

ABSTRACT: Low porosity and permeability of oil and gas reservoirs make it difficult to develop these resources. To address these problems, we developed and evaluated a novel, environmentally friendly waterproof locking agent, which was prepared using dimethyl silicone oil and octadecyltrimethylammonium chloride and characterized by Fourier transform infrared spectroscopy, X-ray photoelectron spectroscopy, and particle size measurement. The waterproof locking performance of the agent was evaluated in a low-permeability reservoir using surface tension and contact angle measurements, and thermodynamic calculations were performed. The average particle size or median diameter (D_{50}) of a 1% mother liquor was 325 nm at 20 °C and 470.8 nm at 70 °C. The contact angle of clean water on the core surface increased from 10 to 110°. At 70 °C, the surface tension of water was reduced to 24 mN·m^{-1}, indicating good waterproof locking performance. The interaction parameters were calculated in accordance with the Langmuir adsorption theory. The increase in temperature from 20 to 70 °C reduced Γ_{max} from 4.59 × 10^{-6} to 1.36 × 10^{-6} mol·m^{-2} and ΔG^{θ} from −40.93 to −56.54 kJ·mol^{-1}. Thus, the adsorption behavior of the developed locking agent is believed to improve the productivity of oil wells.

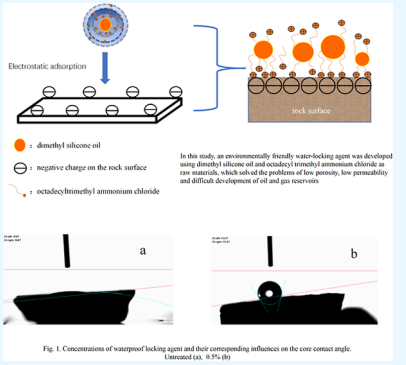

1. INTRODUCTION

Developing low-permeability reservoirs with low porosity and permeability remains a significant challenge owing to the high reservoir stresses and poor water injection effects; both factors are sensitive to water and lead to a water-locking effect.[1,2] This in turn reduces the water injection capacity and quantity of reservoirs near wells and oil-water transition zones, thus reducing the productivity of oil wells.[3]

The addition of a waterproof locking agent to the drilling fluid effectively overcomes the water-locking effect and reduces the wettability of reservoir cores.[4−6] Waterproof locking agents are typically surfactants with a hydrophilic head and a hydrophobic tail.[7] The positive charge on cationic surfactants can affect the adsorption of the head at the oil−water interface of a low-permeability reservoir core. In contrast, a negative surface charge on the surfactant suppresses the hydration expansion of altered clay[8] and simultaneously induces the wettability reversal effect in the reservoir core. When the core contact angle is greater than 90°, the resulting tension tends to outwardly repel the external body in the pore throat.[9] This significantly weakens the self-imbibition effect of reservoir cores, reducing both the capillary force imparted on the solution and the self-imbibition of the pore throat, thereby alleviating the water-locking effect.[10−12] Fluorinated surfactants are effective waterproof locking agents owing to their ability to reduce the surface tension of water from 70 mN·m^{-1}[13] to less than 20 mN·m^{-1},[14] thereby minimizing formation damage and extending the reservoir lifetime in low-permeability reservoirs.[15] Aminnaji et al.[16] studied the wettability of carbonate and sandstone cores treated with fluorinated chemicals, using contact angle measurement, scanning electron microscopy (SEM), and energy dispersive X-ray analysis, and observed altered liquid wetting by increasing surface roughness and decreasing surface free energy. However, fluorinated surfactants are expensive, exhibit poor biodegradability, and readily accumulate in the environment. It is therefore important to find inexpensive, environmentally friendly alternatives to fluorinated surfactants.[17] The use of a single surfactant in low-permeability reservoirs is restricted by high costs stemming from its high adsorption and injection characteristics. Meanwhile, complex binary systems have good application prospects owing to their superior emulsification ability, wettability, and low cost.[18−21]

In this study, we developed a new waterproof locking agent based on a dimethyl silicone oil−octadecyltrimethylammo-

Received: May 9, 2022
Accepted: August 22, 2022
Published: September 1, 2022

© 2022 The Authors. Published by American Chemical Society

nium chloride binary compound. The solution surface tension, contact angle, and reverse wetting ability of this agent on the core surface were investigated using SEM, an integrated analysis method. The calculated thermodynamic properties of the binary compound system elucidated the adsorption behavior of the aqueous solution and explained the performance of the waterproof locking agent.

2. MATERIALS

2.1. Preparation of Cationic Waterproof Locking Agent. All reagents were of analytical grade and purchased from Sinopharm Chemical Reagent Co. Ltd. Deionized water was prepared in the laboratory.

The mother liquor of the cationic waterproof locking agent, which is used in low-permeability reservoirs, was obtained by adding dimethyl silicone oil (4.5 g; molecular weight = 9400 Da, viscosity = 200 cSt, relative density = 0.963 g·cm^{-3}) and octadecyltrimethyl ammonium chloride (0.5 g solid; relative density = 0.884 g·cm^{-3}) (Figure 1) to deionized water (495 mL) and stirred for 10 min in a high shear emulsifying dispersion machine (3000 r/min) to ensure complete dispersion.

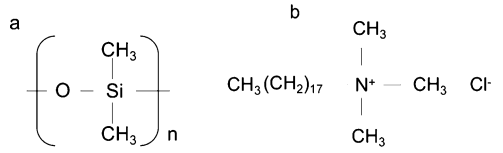

Figure 1. Molecular structure of raw materials: (a) dimethyl silicone oil and (b) octadecyltrimethyl ammonium chloride.

The prepared waterproof locking agent was stirred at 70 °C for 12 h in a 250 mL three-necked flask using a heat-collecting, thermostatic heating magnetic stirrer, for aging.

2.2. Analytical Methods. *2.2.1. FTIR Spectroscopy.* The cationic waterproof locking agent (10 mg) and potassium bromide (100 mg) were pressed into a tablet, to which a drop of dimethyl silicone oil was added with a glass rod. The infrared (IR) spectra was recorded using Fourier transform IR (FTIR) spectroscopy, which was performed using a TP-FTIR spectrometer (Nicolli, USA) at wavenumbers between 400 and 4000 cm^{-1}.

2.2.2. Particle Size Analysis. The particle size distribution was measured using a Winner2000ZD laser particle sizer (Jinan Micro-nano Particle Technology Co. Ltd) before and after aging. The analysis ranged from 0.1 to 40 μm at 25 °C.

2.2.3. XPS Characterization. The natural core was pulverized, and the powder (1 g) was added to a 1% mother liquor (50 ml), in a conical flask, and soaked for 8 h. Afterward, the powder was transferred to a Petri dish and dried in a vacuum drying oven at 50 °C for 12 h. The dried powder was characterized via XPS using an ESCALAB 250Xi XPS photoelectron spectrometer (Thermo Fisher Scientific) under the energy resolution limit of 0.43 eV (the energy analysis range is 0−5000 eV; the pass energy range is 1−400 eV).

2.2.4. Surface Tension Measurement. A portion of the waterproof locking agent was diluted to a concentration of 0.01−1% and heated at 70 °C for 15 min before being quickly transferred into the tensiometer sample cup for surface tension measurements. After cooling to room temperature, the surface tension was measured using the ring method. The surface tension was measured using a JK99B automatic tension meter (Shanghai Wang Xu Electric Co. Ltd); measuring range: 0−500 mN·m^{-1}; sensitivity: 0.01 mN·m^{-1}; accuracy: 0.01 mN·m^{-1}; resolution: 0.01 mN·m^{-1}.

2.2.5. Pretreatment of Natural Core and the Measurement of Contact Angle. The natural core provided by Sinopec Henan Oilfield (mudstone; average porosity = 3.085−14.12%, average permeability = (0.5−24.94) × 10^{-3} μm^2, and average pore throat diameter = 2−30 μm) was broken into 1 cm^3. Both sides of the core were smoothed with 1200-grit sandpaper before being soaked in different concentrations of the waterproofing agent for 8 h in a beaker covered with plastic wrap. The stones were gently removed using tweezers and left in a shaded area for 48 h before contact angle measurements were taken.

The contact angle was measured using an OCA15EC contact angle surface performance tester (Data Physics Corporation, Germany) (the contact angle measurement range: 0−180°, measurement accuracy: ± 0.1°, resolution: ± 0.01°).

3. RESULTS AND DISCUSSION

3.1. FTIR Spectral Analysis of Waterproof Locking Agent. The FTIR spectrum of the treated core surface (Figure 2) exhibits peaks in the range of 2800−3000 cm^{-1}, which are

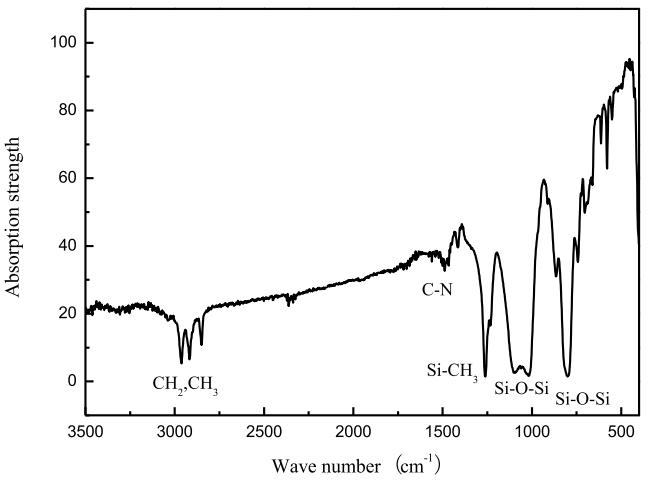

Figure 2. Infrared spectra of the treated core surface.

attributed to the CH_2 and CH_3 stretching vibrations. The peaks at 1472 and 1257 cm^{-1} are due to the C−N stretching and Si−CH_3 deformation vibrations, respectively, while those at 1000−1100 and 800 cm^{-1} are attributed to the Si−O−Si stretching and Si−O−Si bending vibrations, respectively.

3.2. Particle Size Analysis. The particle size of the waterproof locking agent needs to be small enough to enter the core pores and exert its effect. Therefore, it is necessary to investigate the particle size and distribution of the waterproof locking agent. The size distribution of the micellar particles of the waterproof locking agent is narrow and unimodal and reaches the nano level (Figure 3). The D_{50} values at 20 and 70 °C were 325 and 470.8 nm, respectively, owing to an increase in the Brownian motion of the oil-in-water droplets in the waterproof locking agent; as a result of increased temperature, there is a consequent increase in the number and probability of collisions between droplets, leading to an increase in particle size. The average diameter of the low-permeability pore throat is larger than that of the waterproof locking agent at 0.15−4.18

https://doi.org/10.1021/acsomega.2c02878
ACS Omega 2022, 7, 31954−31960

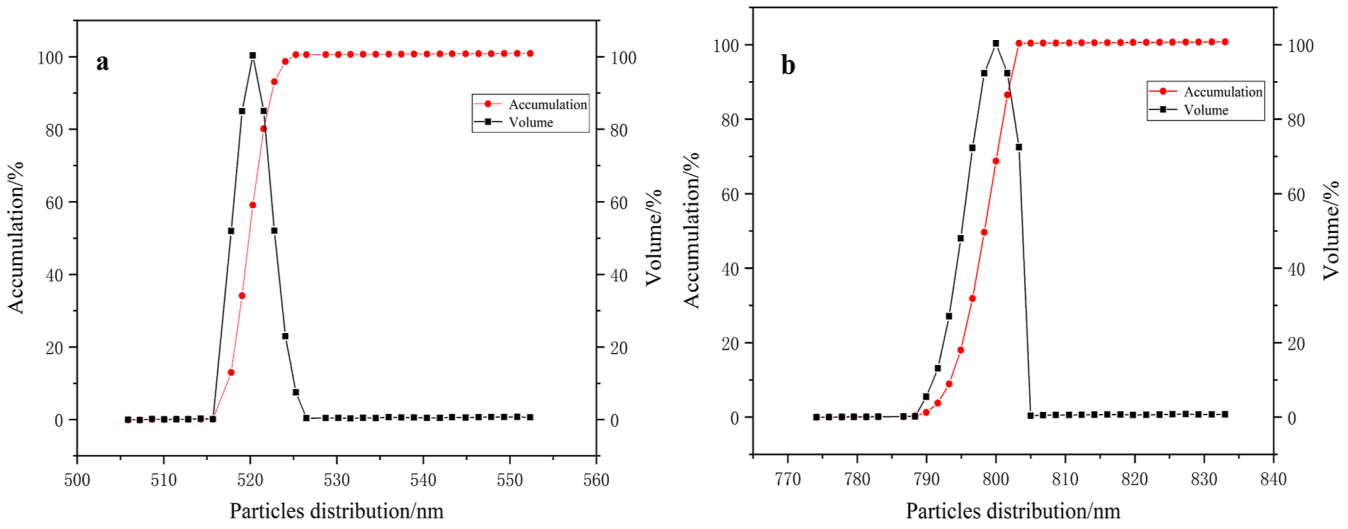

Figure 3. Particle size distribution for 1% emulsion at (a) 20 °C and (b) 70 °C.

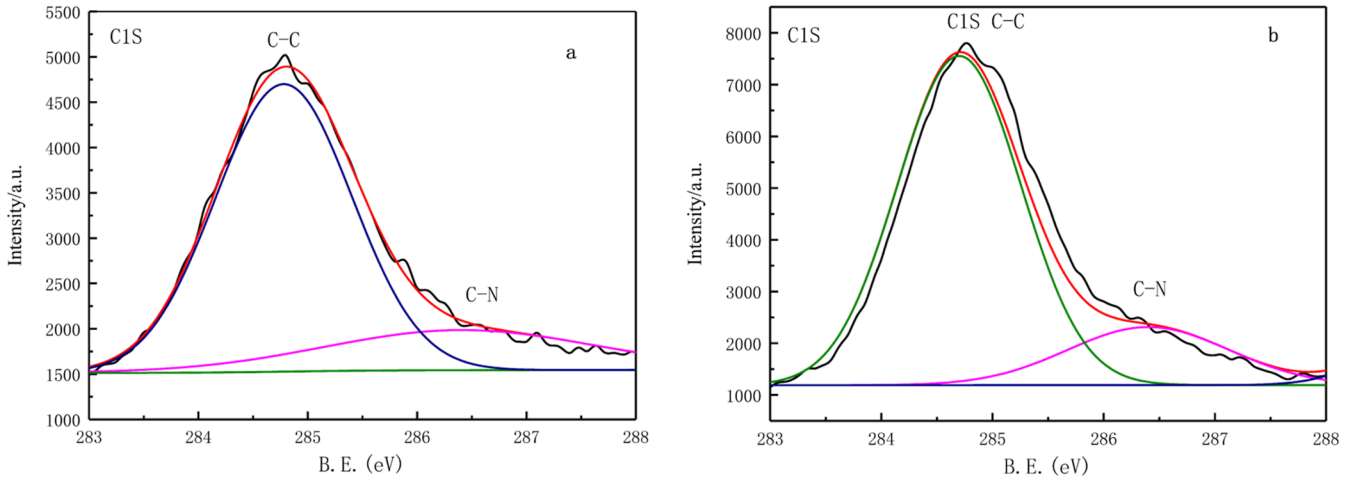

Figure 4. XPS spectra of the core (a) before and (b) after treatment.

μm,[19] allowing the waterproof locking agent to enter the pore throat of the low-permeability reservoir and reduce water lock damage.

3.3. XPS Analysis of Elemental Carbon on the Core Surface. By examining the changes in surface characteristic elements, or groups before and after core treatment, a judgement can be made as to whether the waterproof locking agent is adsorbed onto the core surface or not. The XPS profiles of the core powder before and after treatment with the waterproof locking agent are shown in Figure 4. The binding energy of the C 1s orbital of the core powder is split into two signal peaks at 284.8 and 286.4 eV, attributable to carbon pollution and the C atom (C−N), respectively. The untreated core powder also contains C−N bonds, confirming that the core contains organic matter.[20] The C 1s content increased from 84.19% to 91.69% after the core powder was processed (Table 1), indicating that the ionic surfactant successfully adsorbed onto the surface of the core powder.

3.4. Surface Tension Evaluation. *3.4.1. Effect of Temperature on Surface Tension at the Surfactant−Polymer Interface.* Waterproof locking agents can effectively reduce the surface tension of the wellbore working fluid, weaken the hydration expansion, reduce the diameter of the pore throat, and finally reduce the capillary force of the external fluid invading the pore throat of the reservoir. Figure 5 shows that the waterproof locking agent has high surface activity at low concentrations. However, the surface tension decreases with increasing locking agent concentration, reaching a minimum of 24 $mN \cdot m^{-1}$ at 70 °C (the formation temperature at the core collected in Henan Oilfield). The surface tension of the waterproof locking agent decreases with increasing temperature because the mobility of the molecules increases with temperature, and the cationic surfactants reach the micellar concentration. The newly formed micelles tend to migrate to the surface of the solution, thereby reducing the surface tension.

Table 1. XPS Data of Surface Elements

name	untreated atomic %	treated atomic %
C 1s	84.19	91.69
N 1s	12.79	6.86

The linear fit (Figure 6) for $C/\Gamma - C$ was produced according to the fitting equations: $Y = 43.41710.653 \ln(C + 0.05)$ at 20 °C and $Y = 30.274 - 3.872 \ln(C + 0.005)$ at 70 °C. The maximum adsorption capacity, Γ_{max}, and thermodynamic constant, K, were calculated by eq 3[21,22] and are listed in Table 2.

https://doi.org/10.1021/acsomega.2c02878
ACS Omega 2022, 7, 31954−31960

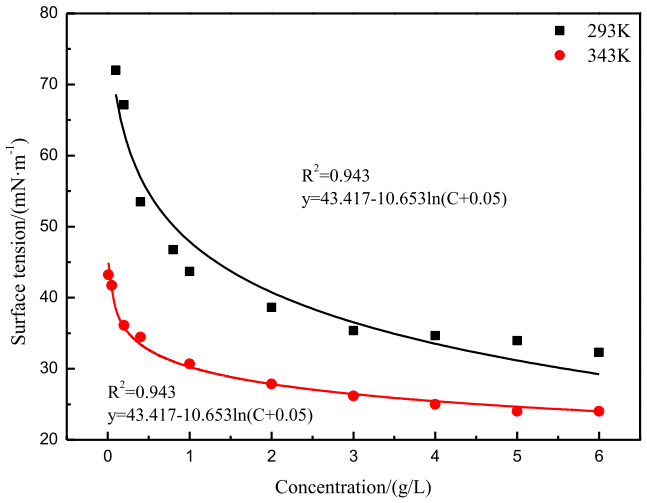

Figure 5. Surface tension of the waterproof locking agent at 20 and 70 °C.

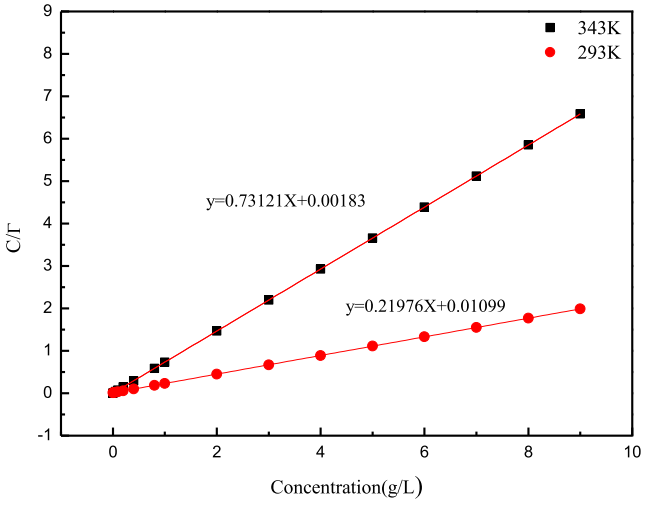

Figure 6. $C/\Gamma - C$ linear fit of waterproof locking agent at 20 and 70 °C.

3.5. Contact Angle Evaluation. Through the investigation of the contact angle, we can qualitatively understand the change of the contact angle between the hydrophilic fluid and the shale, after the water-blocking agent is adsorbed on the core, and analyze its effect on the protection of oil and gas reservoirs. Contact changes on the core surface before and after treatment with the waterproof locking agent are shown Figure 7. The surface of the untreated cores appeared granular and contained numerous micropores. After the core was treated with the waterproof locking agent, dimethyl silicone oil was adsorbed onto the surface of the core particles. Notably, increasing the concentration of the waterproof locking agent resulted in the gradual adsorption of the oil onto the surface of the flake-like polymer core in a net-like fashion. This reduced the surface energy of the core and increased the water contact angle on the core surface. However, at a waterproof locking agent concentration of 0.7%, multimolecular adsorption occurred, thus reducing the contact angle.

The data in Table 3 show that the contact angle of the hydrophilic core surface increases to 114° with increasing waterproof locking agent concentration, indicating an excellent wetting reversal ability.[23] The contact angle first increases and then decreases because the adsorption density of the cationic waterproof locking agent emulsion increases, which changes the spatial arrangement of molecules from a flat single-layer to a horizontal double-layer (Figures 8 and 9).[24,25] The waterproof locking agent also enhanced the hydrophilicity and reduced the contact angle of the surface.

3.7. Evaluation of Performance after Aging. *3.7.1. Evaluation of Surface Tension after Aging.* On application in the field, the waterproof locking agent had a long working time in the underground reservoir. Therefore, the surface tension of the waterproof locking agent, at different concentrations and temperatures, was tested after stirring and aging for 12 h. It can be seen from Figure 10 that the surface tension of the surfactant is around 30 mN·m^{-1} at room temperature and then drops to around 23 mN·m^{-1} at 70 and 80 °C. The surface tension of the aqueous surfactant solution is almost identical, indicating that the high temperature has little effect on the system, and waterproof locking retains good surface activity after aging.

3.7.2. Evaluation of the Contact Angle after Aging. Figure 11 and Table 4 show the static contact angle after aging at 70 °C for 12 h. The contact angle of the hydrophilic core surface increased from 10° to 117° with increasing waterproof locking agent concentration. The effect is similar before aging, demonstrating the high wetting inversion performance of the waterproof locking agent and thus aging resistance.

4. CONCLUSIONS

A novel waterproof locking agent was prepared without the use of fluorine compounds. The agent reached the nano level in water with a D_{50} value of 470.8 nm at 70 °C. The surface tension reached a minimum of 24 mN·m^{-1} at 70 °C. Treatment of the surface of the hydrophilic core with a surfactant increased the contact angle to more than 90°, demonstrating excellent wettability and reversal abilities.

The surface adsorption of the cationic waterproof locking agent emulsion follows a Langmuir-type adsorption isotherm. According to thermodynamic calculations, an increase in temperature reduces the amount of adsorption onto the surface of the emulsion, the area occupied by the emulsion surface molecules, and the thickness of the adsorption layer. The Gibbs free energy values were negative, showing that the adsorption of the waterproof locking agent on the surface is spontaneous under standard conditions.

$$\gamma = \gamma_0' - \gamma_0 b \ln(c + a) \quad (1)$$

$$\Gamma = -\frac{c}{RT}\left(\frac{\partial \gamma}{\partial c}\right)_T \quad (2)$$

Table 2. Calculated Adsorption Properties of the Waterproof Locking Agent

temperature/°C	$\Gamma_{max}/(10^{-6}$ mol·m$^{-2})$	$A_{min}/100$ nm^2	ΔG^θ/kJ·mol^{-1}	δ/nm
20	4.59	36.19	−40.93	74.54
70	1.36	122.14	−56.54	22.08

https://doi.org/10.1021/acsomega.2c02878
ACS Omega 2022, 7, 31954−31960

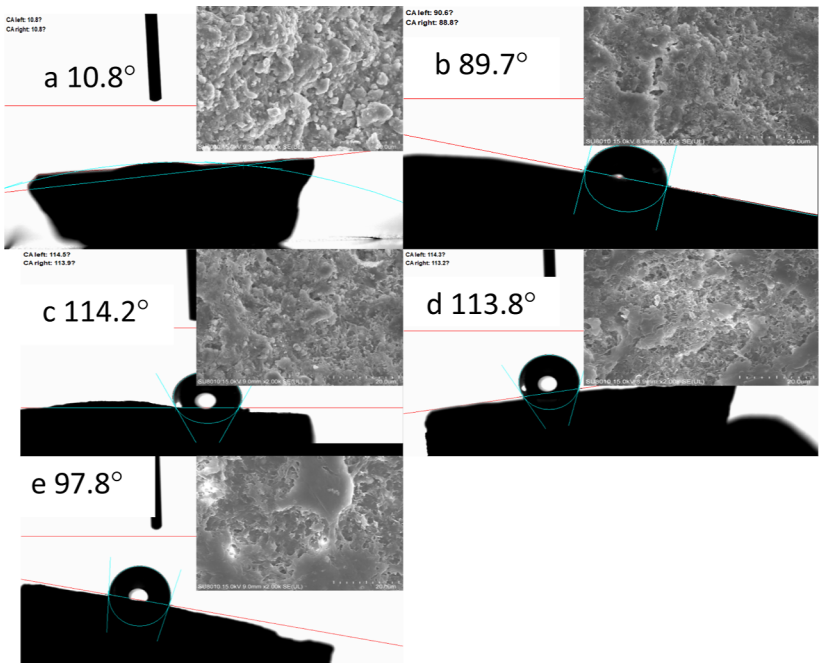

Figure 7. Effect of the waterproof locking agent concentration on the water contact angle of the core: (a) untreated, (b) 0.1%, (c) 0.3%, (d) 0.5%, and (e) 0.7%.

Table 3. Contact Angles before and after Treatment of the Core with the Waterproof Locking Agent

	static contact angle/°			dynamic contact angle/°				
mass/%	left	right	average	left	right	advancing contact angle	receding contact angle	contact angle hysteresis
0	10.80	10.80	10.80					
0.1	90.60	88.80	89.70	84.73	85.15	1.58	0.02	1.56
0.3	114.50	113.90	114.20	109.21	107.31	1.64	0.47	1.17
0.5	114.30	113.20	113.75	116.08	117.50	0.35	0.03	0.32
0.7	96.80	98.90	97.85	109.01	106.57	0.967	0.90	0.06

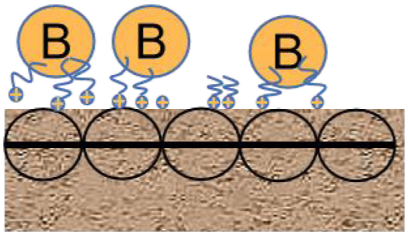

Figure 8. Schematic of a low-concentration waterproof locking agent adsorbed onto the core (B is a low interfacial energy polymer).

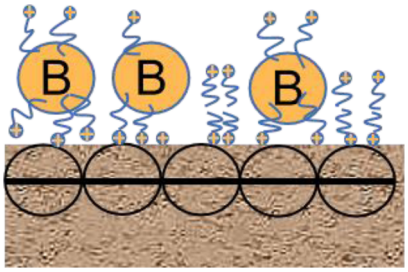

Figure 9. Schematic of a high-concentration waterproof locking agent adsorbed onto the core (B is a low interfacial energy polymer).

$$\frac{c}{\Gamma} = \frac{c}{\Gamma_{max}} + \frac{1}{k\Gamma_{max}} \quad (3)$$

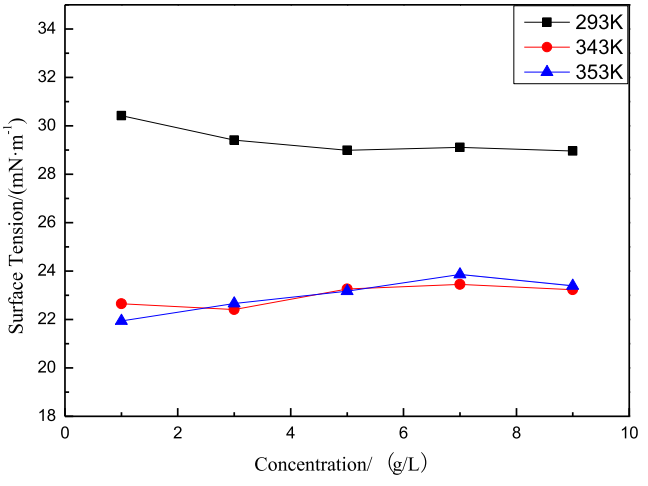

Figure 10. Surface tension test of the surfactant at different temperatures after aging.

$$\Delta G^{\theta} = -RT \ln K \quad (4)$$

$$\delta = \frac{\Gamma_{max} M}{\rho} \quad (5)$$

https://doi.org/10.1021/acsomega.2c02878
ACS Omega 2022, 7, 31954−31960

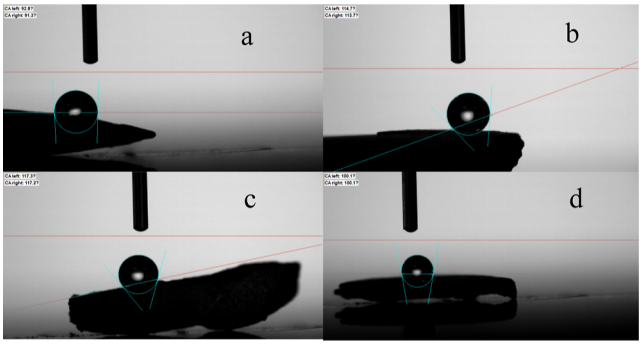

Figure 11. Influence of the waterproof locking agent concentration on the core contact angle after aging: (a) 0.1%, (b) 0.3%, (c) 0.5%, and (d) 0.7%.

Table 4. Contact Angles before and after the Core was Treated with the Waterproof Locking Agent, after Aging

	static contact angle/°		
mass/%	left	right	average
0	10.80	10.80	10.80
0.1	92.80	91.30	92.05
0.3	114.70	113.70	114.20
0.5	117.30	117.20	117.25
0.7	100.10	100.10	100.10

$$A_{min} = \frac{10^{18}}{N_0 \Gamma_{max}} \quad (6)$$

A_{min} is the smallest area occupied by surfactant molecules at the gas−liquid interface, nm^2. C is the surfactant bulk concentration, gL^{-1}. ΔG^{θ} is the standard free energy of adsorption, $kJmol^{-1}$. K is the adsorption equilibrium constant. M is the molecular weight, 16 239 $gmol^{-1}$. N_0 is Avogadro's constant, 6.02×10^{23}. R is the gas constant, 8.314 J $mol^{-1}{\cdot}K^{-1}$. T is the temperature, K. Γ is the surface tension, $mN{\cdot}m^{-1}$. ρ is the liquid density, kg m^{-3}. δ is the saturated adsorption layer thickness, nm. Γ_{max} is the saturated adsorption capacity, mol m^{-2}. Constants related to a, b. a, b empirical constants in Siskowski's empirical formula.

AUTHOR INFORMATION

Corresponding Authors

Xiaolong Zhao − *Petrochemical College, Liaoning Petrochemical University, Fushun 113001 Liaoning, China;* orcid.org/0000-0002-5793-3122; Phone: 13842382945; Email: 184348285@qq.com

Cheng Ma − *Petrochemical College, Liaoning Petrochemical University, Fushun 113001 Liaoning, China;* Phone: 18841322939; Email: kkmc2002@163.com

Authors

Miao Liu − *Petrochemical College, Liaoning Petrochemical University, Fushun 113001 Liaoning, China; PetroChina Liaoyang Petrochemical Company, Liaoyang 111000 Liaoning, China*

Chen Wang − *Sinopec Dalian (Fushun) Research Institute of Petroleum and Petrochemicals, Dalian 116045 Liaoning, China*

Jiang Yang − *Petrochemical College, Liaoning Petrochemical University, Fushun 113001 Liaoning, China*

Chao Yang − *Sinopec Dalian (Fushun) Research Institute of Petroleum and Petrochemicals, Dalian 116045 Liaoning, China;* orcid.org/0000-0002-8931-5070

Zhongwei Sun − *Engineering Institute of Sinopec Henan Oilfield Company, Nanyang 473132 Henan, China*

Complete contact information is available at: https://pubs.acs.org/10.1021/acsomega.2c02878

Author Contributions

The manuscript was written with contributions from all authors. All authors have given approval for the final version of the manuscript. X.Z. drafted the main part of the paper and was responsible for the planning, implementation, and modification of the entire experiment. M.L. participated in the experiment and analyzed the experimental results. C.M., C.W., J.Y., C.Y., and Z.S. coordinated the study and reviewed the manuscript. C.M. and J.Y. provided financial help.

Funding

This project was funded by the Development and application of environmentally friendly starch-based drilling fluid treating agent [contract number 219032-3] and "Xingliao Talents" program of the Liaoning Province, China, under grant no. SLYC1902053.

Notes

The authors declare no competing financial interest.

The authors confirm that the data supporting the findings of this study are available within the article and its supplementary materials.

ACKNOWLEDGMENTS

We are grateful to M.L. for typing the manuscript. We also greatly appreciate Prof. Yang for the helpful discussion. We would like to thank Editage (www.editage.cn) for English language editing.

REFERENCES

(1) Wenrui, H.; Yi, W.; Jingwei, B. Development of the theory and technology for low permeability reservoirs in China. *Pet. Explor. Dev.* **2018**, *45*, 125−137.

(2) Liang, T. B.; Gu, F. Y.; Yao, E. D.; Zhang, L.; Yang, K.; Liu, G.; Zhou, F. Formation damage due to drilling and fracturing fluids and its solution for tight naturally fractured sandstone reservoirs. *Geofluids* **2017**, *2017*, 9350967.

(3) Wang, L.; Zhang, H.; Peng, X.; Wang, P.; Zhao, N.; Chu, S.; Wang, X.; Kong, L. Water-sensitive damage mechanism and the injection water source optimization of low permeability sandy conglomerate reservoirs. *Pet. Explor. Dev.* **2019**, *46*, 1218−1230.

(4) Xu, D.; Li, Z.; Bai, B.; Chen, X.; Wu, H.; Hou, J.; Kang, W. A systematic research on spontaneous imbibition of surfactant solutions for low permeability sandstone reservoirs. *J. Pet. Sci. Eng.* **2021**, *206*, 109003.

(5) Ding, B.; Xiong, C.; Geng, X.; Guan, X.; Pan, B.; Xu, J.; Dong, J.; Zhang, J.; Zhang, C. Characteristics and EOR mechanisms of nanofluids permeation flooding for tight oil. *Pet. Explor. Dev.* **2020**, *47*, 810−819.

(6) Wang, Y.; Jin, J.; Ma, L.; Li, L.; Zhao, X. Influence of wettability alteration to preferential Gas-Wetting on displacement efficiency at elevated temperatures. *J. Dispersion Sci. Technol.* **2015**, *36*, 1274−1281.

(7) Chen, W.; Schechter, D. S. Surfactant selection for enhanced oil recovery based on surfactant molecular structure in unconventional liquid reservoirs. *J. Pet. Sci. Eng.* **2021**, *196*, 107702.

(8) Zeng, F.; Zhang, Q.; Guo, J.; Zeng, B.; Zhang, Y.; He, S. Mechanisms of shale hydration and water block removal. *Pet. Explor. Dev.* **2021**, *48*, 752−761.
(9) Alvarez, J. O.; Schechter, D. S. Application of wettability alteration in the exploitation of unconventional liquid resources. *Pet. Explor. Dev.* **2016**, *43*, 832−840.
(10) Yang, Z.; Liu, X.; Li, H.; Lei, Q.; Luo, Y.; Wang, X. Analysis on the influencing factors of imbibition and the effect evaluation of imbibition in tight reservoirs. *Pet. Explor. Dev.* **2019**, *46*, 779−785.
(11) Liu, X.; Kang, Y.; Li, J.; Chen, Z.; Ji, A.; Xu, H. Percolation characteristics and fluid movability analysis in tight sandstone oil reservoirs. *ACS Omega* **2020**, *5*, 14316−14323.
(12) Zhang, D.; Bai, Y.; Shen, J.; Wang, G. Surface activities and wetting behavior of fluorocarbon-cationic and hydrocarbon-anionic surfactant mixtures in dilute solutions. *J. Mol. Liq.* **2019**, *286*, 110947.
(13) Phan, C. M. The surface tension and interfacial composition of water/ethanol mixture. *J. Mol. Liq.* **2021**, *342*, 117505−117508.
(14) Yayayürük, A. E.; Yayayürük, O. Applications of green chemistry approaches in environmental analysis. *Curr. Anal. Chem.* **2019**, *15*, 745−758.
(15) Wang, C.; Wang, Y.; Kuru, E.; Chen, E.; Xiao, F.; Chen, Z.; Yang, D. A New Low-Damage Drilling Fluid for Sandstone Reservoirs With Low Permeability: Formulation, Evaluation, and Applications. *J. Energy Resour. Technol.* **2021**, *143*, 053004.
(16) Aminnaji, M.; Fazeli, H.; Bahramian, A.; Gerami, S.; Ghojavand, H. Wettability Alteration of Reservoir Cores from Liquid Wetting to Gas Wetting Using Nanofluid. *Transp. Porous Media* **2015**, *109*, 201−216.
(17) Wang, W.; Yue, X.; Chen, Y. A laboratory feasibility study of surfactant-polymer combinational flooding in low permeability. *Reservoirs* **2013**, *34*, 639−643.
(18) Yu, Q.; Liu, Y.; Liang, S.; Tan, S.; Sun, Z.; Yu, Y. Experimental study on surface-active polymer flooding for enhanced oil recovery: A case study of Daqing placanticline oil field, NE China. *Pet. Explor. Dev.* **2019**, *46*, 1206−1217.
(19) Azar, E.; Blanc, C.; Mehdi, A.; Nobili, M.; Stocco, A. Mesoporous silica colloids: Wetting, surface diffusion, and cationic surfactant adsorption. *J. Phys. Chem. C* **2019**, *123*, 26226−26235.
(20) Guan, Q.; Dong, D.; Zhang, H.; Sun, S.; Zhang, S.; Guo, W. Types of biogenic quartz and its coupling storage mechanism in organic-rich shales: A case study of the Upper Ordovician Wufeng Formation to Lower Silurian Longmaxi Formation in the Sichuan Basin, SW China. *Pet. Explor. Dev.* **2021**, *48*, 813−823.
(21) Qin, L.; Wang, X. Surface adsorption and thermodynamic properties of mixed system of ionic liquid surfactants with cetyltrimethyl ammonium bromide. *RSC Adv.* **2017**, *7*, 51426−51435.
(22) Jin, G. U. *Surfactant Chemistry*, 2nd ed.; University of Science and Technology of China Press, 2013; pp. 50−70.
(23) Ren, X.; Liu, N. Effect of wettability alteration on the relative permeability of low-permeability water-wet oil and gas reservoirs. *Pet. Explor. Dev.* **2005**, *32*, 123−126.
(24) Mao, J.; Wang, D.; Yang, X.; Zhang, Z.; Yang, B.; Zhang, Z. C. Adsorption of surfactant on stratum cores: Exploration of low adsorption surfactants for reservoir stimulation. *J. Taiwan Inst. Chem. Eng.* **2019**, *95*, 424−431.
(25) Andrunik, M.; Bajda, T. Modification of bentonite with cationic and nonionic surfactants: Structural and textural features. *Materials* **2019**, *12*, 3772.

https://doi.org/10.1021/acsomega.2c02878
ACS Omega 2022, 7, 31954−31960